PV Power Optimization with Dual Winding Step-Up Converter and Woodpecker Mating Algorithm Based Cascaded ANN MPPT

Amar K.T., Gowthami K., Sridhar Madireddy, Mohan S.D.R.M., Manikanth L.

School of Engineering, Godavari Institute of Engineering and Technology (A), Rajahmundry, India

***Abstract*.** The main objectives of this study are to enhance the power extraction of photovoltaic (PV) systems under rapidly changing ecological circumstances using Maximum Power Point Tracking (MPPT) and to improve the power quality of grid connected renewable energy systems (RESs) via developing an intelligent high-gain energy conversion architecture. These objectives are achieved by designing a PV energy conversion system using an extended dual winding (X^2W) step-up converter and an intelligent optimized MPPT method for efficient integration with the utility grid connected systems. The X^2W step up converter is employed for enhancing high voltage gain from low-output PV Module. The Woodpecker Mating Algorithm (WMA) based optimization optimally tune the parameters of cascaded artificial neural network (CANN) MPPT, which improved the convergence speed and accurate tracking under dynamic weather condition. A three-phase voltage source inverter (3φ VSI) is employed for converting DC to AC power, enabling effective integration with utility grids. The most important results are that the proposed system achieves exceptional tracking accuracy, a shortened convergence time, better dynamic stability during load and grid disturbances, increased voltage boosting performance, and a highest power conversion efficiency of 94.84%, verified by simulation studies carried out on the MATLAB and Simulink platform. The significance of the obtained results lies in offering a stable, scalable, and intelligent control solution for modern PV grid connected systems, increasing the overall system efficiency, lowering energy losses, enhancing the operational reliability of future sustainable power networks, and facilitating the evolution of next-generation smart energy infrastructures.

***Keywords*:** photovoltaic, Maximum Power Point Tracking, X^2W step-up converter, cascaded artificial neural network, Woodpecker Mating Algorithm, three-phase voltage source inverter.

DOI: https://doi.org/10.52254/1857-0070.2026.2-70.02
UDC: 621.31.04

Optimizarea puterii fotovoltaice cu convertor elevator de tensiune cu două înfășurări și MPPT ANN în cascadă bazat pe algoritmul de cuplare Woodpecker

Amar K.T., Gowthami K., Sridhar Madireddy, Mohan S. D. R. M., Manikanth L.

Institutul de Inginerie și Tehnologie Godavari (A), Rajahmundry

Rezumat. Principalele obiective ale acestui studiu sunt de a îmbunătăți extracția de energie a sistemelor fotovoltaice (PV) în circumstanțe ecologice în rapidă schimbare, utilizând urmărirea punctului de putere maximă (MPPT) și de a îmbunătăți calitatea energiei sistemelor de energie regenerabilă (RES) conectate la rețea prin dezvoltarea unei arhitecturi inteligente de conversie a energiei cu câștig ridicat. Aceste obiective sunt atinse prin proiectarea unui sistem de conversie a energiei fotovoltaice utilizând un convertor step-up extins cu înfășurare dublă ( ) și o metodă MPPT optimizată inteligent pentru integrarea eficientă cu sistemele conectate la rețeaua utilităților. Convertorul step-up este utilizat pentru a îmbunătăți câștigul de tensiune ridicată de la modulul fotovoltaic de putere redusă. Optimizarea bazată pe algoritmul de cuplare Woodpecker (WMA) reglează optim parametrii MPPT ai rețelei neuronale artificiale în cascadă (CANN), ceea ce a îmbunătățit viteza de convergență și urmărirea precisă în condiții meteorologice dinamice. Un invertor de tensiune trifazat (3 VSI) este utilizat pentru convertirea energiei continue în curent alternativ, permițând integrarea eficientă cu rețelele utilităților. Cele mai importante rezultate sunt că sistemul propus atinge o precizie excepțională de urmărire, un timp de convergență scurtat, o stabilitate dinamică mai bună în timpul sarcinii și a perturbațiilor rețelei, performanțe sporite de amplificare a tensiunii și o eficiență maximă a conversiei de putere de 94,84%, verificată prin studii de simulare efectuate pe platforma MATLAB și Simulink. Semnificația rezultatelor obținute constă în oferirea unei soluții de control stabile, scalabile și inteligente pentru sistemele fotovoltaice moderne conectate la rețea, creșterea eficienței generale a sistemului, reducerea pierderilor de energie, îmbunătățirea fiabilității operaționale a viitoarelor rețele energetice sustenabile și facilitarea evoluției infrastructurilor energetice inteligente de generație următoare.

Cuvinte-cheie: fotovoltaic, urmărirea punctului de putere maximă, convertor Step-Up , rețea neuronală artificială în cascadă, algoritmul de Împerechere Woodpecker, invertor trifazat de tensiune.

Оптимизация мощности фотоэлектрических систем с помощью двухобмоточного повышающего преобразователя и каскадного алгоритма сопряжения Woodpecker на основе искусственной нейронной сети для отслеживания точки максимальной мощности

Амар К.Т., Гоутами К., Шридхар М., Мохан С. Д. Р. М., Маникант Л.
Институт инженерии и технологий Годавари (А), Раджахамдри

Аннотация. Нелинейные характеристики генерации энергии фотоэлектрическими (PV) системами требуют внедрения методов отслеживания точки максимальной мощности (MPPT) для генерации максимально возможной мощности. Традиционные подходы MPPT демонстрируют низкую производительность, особенно при динамически меняющихся условиях окружающей среды. Следовательно, в данной статье предлагается система преобразования энергии PV с использованием повышающего преобразователя с расширенной двойной обмоткой (X^2 Вт) и интеллектуального оптимизированного метода MPPT для систем, объединенных в сеть. Повышающий преобразователь X^2 Вт используется для повышения коэффициента усиления высокого напряжения от маломощного фотоэлектрического модуля. Оптимизация на основе алгоритма сопряжения Woodpecker (WMA) оптимально настраивает параметры MPPT каскадной искусственной нейронной сети (CANN), что улучшает скорость сходимости и точность отслеживания в динамических погодных условиях. Для преобразования постоянного тока в переменный используется трехфазный инвертор напряжения (3φVSI), что обеспечивает эффективную интеграцию с коммунальными сетями. Экспериментальная проверка в MATLAB/Simulink показывает, что предлагаемая архитектура обеспечивает повышение эффективности преобразователя на 94,84%, динамическую устойчивость и оптимальный усилитель мощности, а также подходит для интеграции современных фотоэлектрических сетей с интеллектуальной оптимизацией.

Ключевые слова: фотоэлектрические системы, отслеживание точки максимальной мощности, повышающий преобразователь мощностью X^2 Вт, каскадная искусственная нейронная сеть, алгоритм Woodpecher, трехфазный инвертор напряжения.

I. INTRODUCTION

The economic growth and rising energy consumption have made the demand for clean, and maintainable energy source is crucial. Therefore, the RESs like PV systems reduce the greenhouse gas emissions compared to conventional electric generation [1-2] PV technology has been attractive alternative due to the rising demand of electricity, increasing costs and limited supply of fossil fuels. Also, other advantages included by PV systems include availability, zero emissions, and relatively low operation and maintenance cost [3-4].

However, PV systems have intermittency and variability characteristics based on location, time, season, and atmosphere. Therefore, PV sources are inherently low voltage, and thus necessitates a DC-DC converters in the solar systems to raise the voltage level to a usable level [5-6]. Furthermore, to enhance the energy conversion, MPPT controller is crucial component that ensure a PV system activates at its MPP. Nevertheless, this approach failed to offer accurate MPP tracking, resulting in voltage oscillations near to MPP. To address these issues, many researchers have widely developed the optimization approaches to identify global optimum solution through creating random variables in the search spaces [7-8]. In recent years, various converters and optimized controllers are developed for enhancing the performance of the PV and which discussed following section.

Literature Survey

Davut Ertekin *et al* (2023) [9] have developed a high-gain switched-inductor-capacitor DC-DC boost converter with an MPPT controller to enhance output voltage of PV systems, aiming to reduce input current ripple and voltage stress across switches. However, the circuit complexity and component count increase challenges related to cost and thermal management, particularly for commercial-scale implementations. **L. Pirashanthiyah *et al* (2024)** [10] have implemented a three-phase interleaved DC-DC boost converter integrated with a fuzzy logic controlled MPPT system, which aims to improve dynamics, reduce voltage and current ripple, and improve efficiency in PV applications directly integrated into batteries. The absence of experimental verification, rely on simulation results limits the immediate practical applicability and require a hardware implementation to confirm in real-world performance. **Aamir Hayat *et al* (2023)** [11] have presented a non-isolated DC–DC boost converter with MPPT features, in which utilize state-space modeling to design the input

capacitor and optimize dynamic performance in a PV based system. Nevertheless, an oversized input capacitor in relevance to the output capacitor, negatively impacted MPPT efficiency by decreasing system stability and degrading output voltage quality during variational irradiance conditions. **Souheyb Mohammed Belhadj *et al* (2025)** [12] have developed a high-gain Three-Level Quadratic DC-DC Boost Converter (TLQ-DC-DC-BC) combined with a Type-2 Fuzzy Logic Controller (T2FLC) for MPPT, with the aim of improving energy harvesting, reducing oscillations, and enhancing robustness during changing environmental conditions in PV systems. However, this method has not been experimentally validated yet, and it complex for real-time implementations and large-scale applications. **Mohammad Haziq Ibrahim *et al* (2023**) [13] have designed a MPPT controller by combining PSO and Perturb & Observe (P&O) methods with the goal of leveraging the dynamic adjustment of the step size and improved tracking efficiency for grid-tied PV systems. However, this approach is still lacking real-time experimental validation and introduce additional computational overhead. **Majid Dehghani *et al* (2020)** [14] have establishes Genetic Algorithm (GA) optimized FLC to improve MPPT performance in grid-connected PV systems when the atmospheric conditions change rapidly, with the aim to deliver improved response time and tracking accuracy. However, the effectiveness of the controller is limited to a precise tuning of the fuzzy parameters, and the FLC computationally expensive for real-time applications. **Abdulaziz Almutairi *et al* (2020)** [15] have offered an MPPT controller based on the Opposition-based Grey Wolf Optimization (OGWO) algorithm to accurately track the Global Maximum Power Point (GMPP) in PV grid-connected systems in irregular shading situations. It enhances tracking speed and stability, nonetheless it uses complex metaheuristic tuning which increase the implementation complexity. **Mohammed Hassan EL-Banna *et al* (2024)** [16] have employed the Golf Optimization Approach (GOA) as an optimization method with the goal of improving accuracy of MPPT and performance of inverter in grid-tied PV systems under partial shading. Nevertheless, described method involves a higher computational burden and requires close tuning to enable stable performance under rapidly changing conditions. **Efrain Mendez-Flores *et al* (2022)** [17] have utilized an Earthquake Optimization Algorithm (EOA)-based MPPT algorithm and optimally designed DC–DC converter indicated to increase energy harvesting in PV array under changing environmental conditions. However, it lacks closed-loop voltage and current control structure, limiting its ability to maintain steady output and requiring further development for real-time application. **Soroush Esmaeili *et al* (2021)** [18] have implemented step-up coupled dual winding quadratic converter delivers high voltage gain in PV based system. However, this converter limits to control the leakage effect that affect the design of clamping circuit. **Saeed Danyali *et al* (2021)** [19] have presented a dual input three winding coupled inductor to enhance voltage from PV. Nevertheless, its operation requires a careful control of PWM switches and need a stable voltage regulation.

Therefore, in this work, to overcome the limitations of existing systems, a X^2W step up converter integrated with WMA-CANN-MPPT controller is proposed for enhancing PV voltage tracking efficiency and power conversion in PV systems. The distinctive contributions of this work include,

- PV system is converting solar energy into electrical power and supply it for grid integration.
- X^2W step-up converter is utilized to attain higher voltage gain and maximize the efficiency of power conversion.
- WMA is employed to optimize the tuning parameters of CANN-MPPT controller, ensuring a faster convergence and increase tracking efficiency, especially in dynamic environmental conditions.
- A 3 φ grid-connected VSI, along with an LC filter, is integrated to inject the power consistently and synchronously to the utility grid.

II. PROPOSED SYSTEM DESCRIPTIONS

The proposed structure employs a PV array to capture solar energy and extract DC power, enabling efficient conversion and distribution to the grid as illustrates in Fig. 1. An X^2W step-up converter boosts the DC voltage to required levels suitable for grid-tied applications, considering weather factors.

To optimize energy extraction from PV, optimized controller is utilized, incorporating a CANN-MPPT controller which tuned using WMA for effective tracking of the MPP.

The MPP is regulated by generating reference signals that drive PWM generator to control the converter operations.

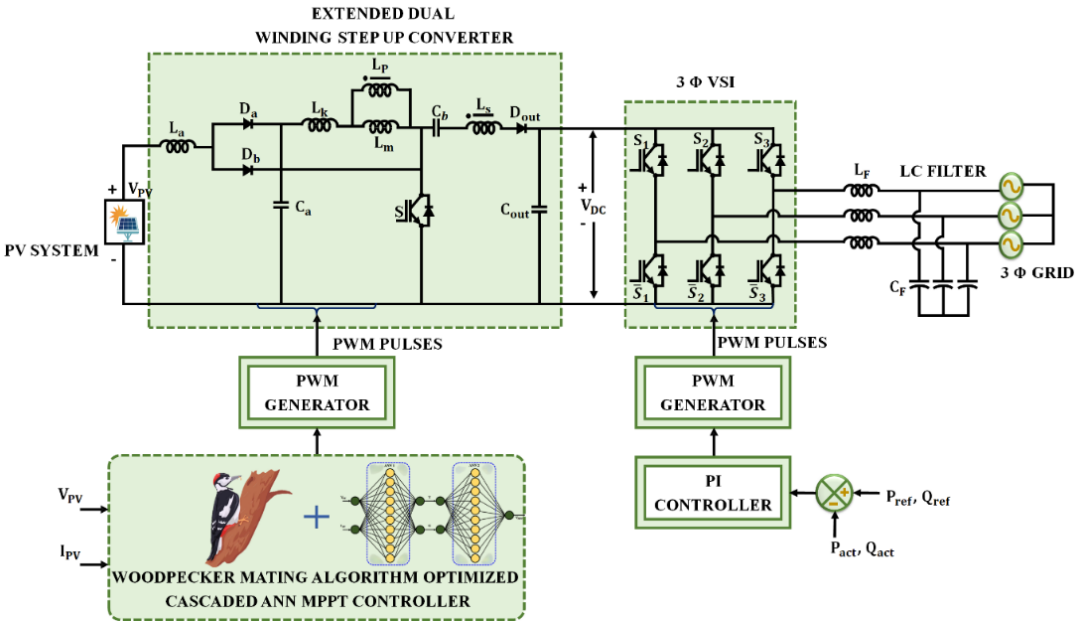

Fig.1. Proposed block of PV integrated grid system using X^2W step-up converter.

The boosted DC power is supplied to a 3 φ VSI that convert the DC power into AC power. VSI output is filtered using an LC filter to reduce the switching harmonics of the VSI output signals. The output to the model is 3 φ AC power which is reliable output into the grid. Thus, the proposed system delivers clean power supply with increased dependability for PV-grid applications.

III. PROPOSED METHODOLOGY

A. PV System

Solar cell is basic unit of PV module and it's responsible for converting UV rays, or photons into electrical power in Fig. 2. It is a $P-N$ junction type, with electrical properties that differ very slightly from a standard diode, as expressed by Shockley's equation (1). Hence, the development of solar cell formulated based on calculations (1), (2) and (3).

$$I_D = I_o \cdot \left[e^{\frac{V_c q}{akT_{ck}}} - 1 \right] \tag{1}$$

Here, I_D stands diode current (A), I_o denotes saturation, V_c stands cell voltage, q stands electron charge, a stands diode ideality constant, k stands Boltzmann's constant, T_{ck} denotes cell temperature. The cell's current is the difference between photocurrent I_L and I_D expressed in formula (2),

$$I = I_L - I_D \tag{2}$$

Substituting (1) into (2) and including series resistance R_s. Thus, the diode voltage is $V_c = V + IR_s$ gives:

$$I = I_L - I_o \cdot \left[e^{\frac{(V+IR_s)q}{akT_{ck}}} - 1 \right] \tag{3}$$

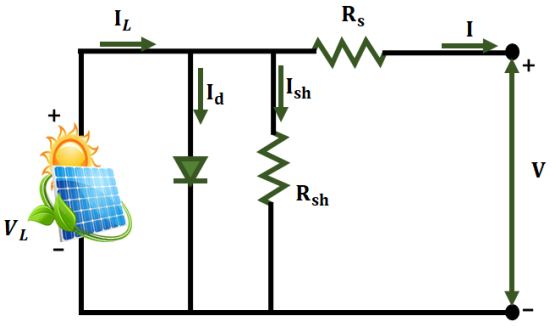

Fig.2. Solar cell diagram.

Include the shunt (parallel) resistance R_{sh} gives throughout the single-diode implicit $I-V$ equation.

$$I = I_L - I_o \cdot \left[e^{\frac{(V+IR_s)q}{akT_{ck}}} - 1 \right] - \frac{V + IR_s}{R_{sh}} \qquad (4)$$

Equation (4) illustrates that the output current generated is dependent upon PV's modules voltage and solar irradiance. Moreover, due to the environmental condition, a DC-DC converter is implemented to enhance voltage level, which is discussed below.

B. Extended Dual Winding Stepup Converter

The topology of the X^2W step-up Converter is to utilize the minimal amount of active and passive components to attain a high voltage conversion gain. The components are as displays Fig. 3, including inductors (L_a), capacitors (C_a, C_b, C_{out}), diode type components (D_a, D_b, D_{out}), coupled inductor is represented as a combination of a magnetizing inductor (L_m) a leakage inductance (L_k), The coupled inductor has two windings primary winding (L_p) and secondary winding (L_s). The modes of operation displays in Fig. 4 (a) and (b).

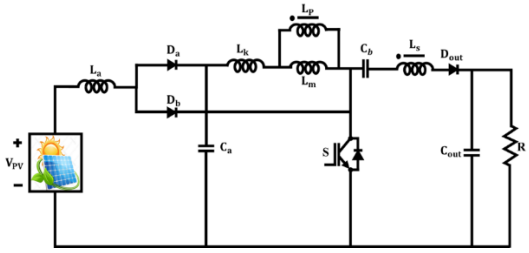

Fig.3. Circuit diagram of proposed converter.

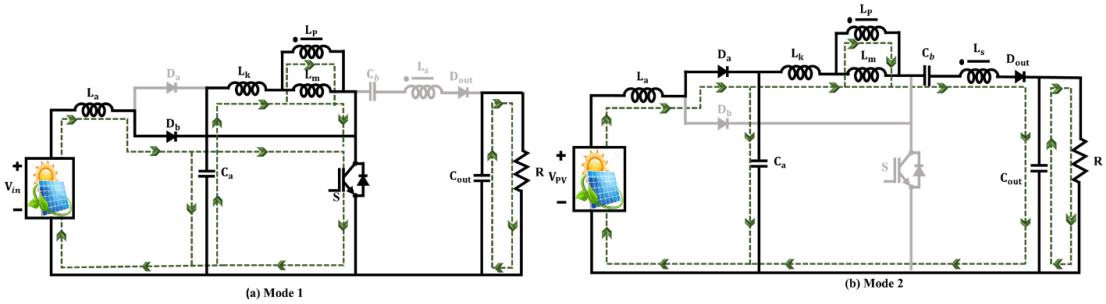

Fig.4. Equivalent circuits for each mode.

Mode 1: In Mode 1, switch *S* and diode D_b are ON, and diodes $D_a, and\ D_{out}$ are OFF. During this time, the input voltage (V_{in}) is providing energy to inductor L_a, which is increasing current linearly to store magnetic energy. At the same time, capacitor C_a has discharged and its stored energy into the primary winding (L_p) of coupled inductor and magnetizing inductor (L_m), which in turn increased the currents through the L_m and leakage inductor (L_k). Capacitor C_b and the secondary winding (L_s) in this mode are inactive consequently the currents are zero. The output capacitor (C_{out}) is discharges its stored energy to the load, maintaining the load voltage, as no energy is being transferred by the active components.

Voltage across inductor L_a :

$$V_{La} = V_{in} \qquad (5)$$

Voltage across inductor L_k and magnetizing inductance L_m :

$$V_{Lk} = V_{Lm} = V_{ca} \qquad (6)$$

Mode 2: Switch S turns OFF and diode D_b becomes reverse-biased in Mode 2. Diode $D_a, and\ D_{out}$ are ON. In this mode, the input source (V_{in}) and energy stored in inductor L_a is recharging capacitor C_a. The capacitor C_a charges until the voltage across $C_a > V_{in}$, producing L_a to have a negative voltage across, which causes the L_a current to decrease linearly. The energies stored in L_a, C_a, L_p, and C_b are transmitted to output through diodes $D_a, and\ D_{out}$. This combined energy transfer charges the output capacitor (C_{out}) and supplies the load to create a significant voltage gain during this time.

Voltage across inductor L_a :

$$V_{La} = V_{in} - V_{ca} \qquad (7)$$

Voltage across the output loop:

$$V_{out} = V_{in} + V_{La} + V_{cb} + n \cdot V_{Lm} \qquad (8)$$

where n represents secondary to primary winding turns ratio of connected inductor. To calculate voltage gain, apply volt-second balance principle to inductors L_a and L_m during an overall switching cycle (T):

Volt-Second Balance on L_a:

$$V_{in} \cdot D + (V_{in} - V_{Ca}) \cdot (1-D) = 0 \quad (9)$$

$$V_{Ca} = \frac{V_{in}}{1-D} \quad (10)$$

Voltage Gain Expression,

$$V_{out} = V_{in} + (V_{in} - V_{Ca}) + V_{Cb} + n \cdot (-V_{Ca}) \quad (11)$$

$$V_{out} = 2V_{in} - V_{Ca}(1-n) + V_{Cb} \quad (12)$$

From capacitor C_b voltage balance derived through charge balance principle:

$$V_{Cb} = \frac{D \cdot V_{in}}{(1-D)^2} \quad (13)$$

$$V_{out} = 2V_{in} - \frac{V_{in}(1+n)}{1-D} + \frac{D \cdot V_{in}}{(1-D)^2} \quad (14)$$

$$V_{out} = V_{in}\left[2 - \frac{2}{1-D} + \frac{D}{(1-D)^2}\right] \quad (15)$$

Thus, the voltage gain (M) becomes:

$$M = \frac{2 - 2D + D^2}{(1-D)^2} \quad (16)$$

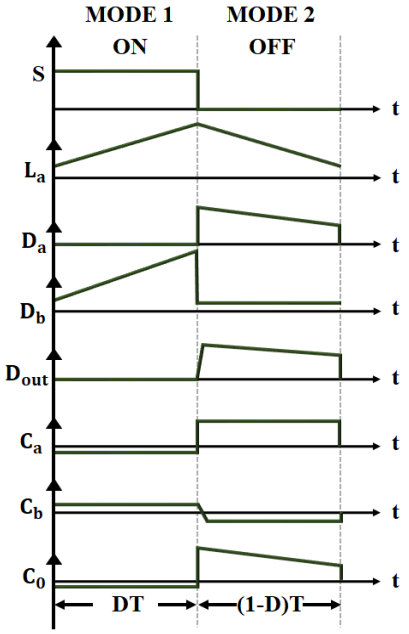

Fig.5. Proposed converter switching waveform.

The timing waveform for line frequency operation as displays in Fig. 5. Proposed converter has favourable characteristics for renewable energy applications including high voltage gain, lower voltage stress across components, and respectable energy transfer via coupled inductors. In addition, to continuously enhance extreme power from the PV source under different ecological conditions an optimized MPPT algorithm is employed.

C. Woodpecker Mating Algorithm Based Cascaded Ann Mppt Controller

Cascaded Ann Mppt Controller

A CANN-based MPPT controller is employed for the purpose of enhancing PV system performance in non-uniform environments. The controller has two ANN models sequentially, directing the estimated values and environmental parameters as shown Fig. 6. The ANN-1, receives V_{PV}, I_{PV}, as PV voltage and current inputs, and develops estimates of solar irradiance G and panel temperature T, by nonlinear mapping:

$$[G,T] = ANN_1(V_{PV}, I_{PV})] \quad (17)$$

The outputs from ANN-1 serve as inputs to the second network ANN-2, which establishes the appropriate MPP voltage V_{MPP} using:

$$V_{MPP} = ANN_2(G,T) \quad (18)$$

Each ANN employs a feedforward architecture using sigmoid activation functions. Therefore, the output of each neuron at the hidden node can be defined as:

$$h_j = \varnothing\left(\sum_{i=1}^{n} w_{ij} x_i + b_j\right), \varnothing(x) = \frac{1}{1+e^{-x}} \quad (19)$$

The final output of the ANN is expressed as:

$$y = \sum_{j=1}^{m} v_j h_i + b_o \quad (20)$$

where x_i denotes input features, w_{ij} and w_{ij} are connection weights, and $b_j and b_o$ are bias terms. The V_{MPP} is estimated and compared to the observed PV voltage providing an error signal, which used to direct the system to the MPP.

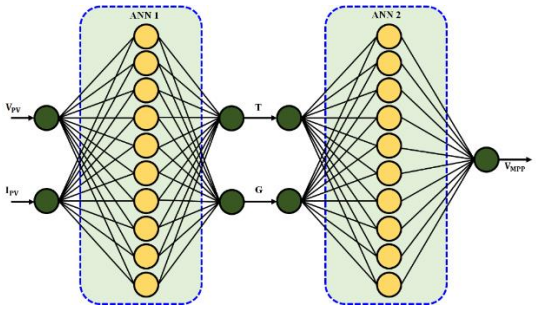

Fig.6. Cascaded ANN MPPT structure.

To achieve improved accuracy tracking and stability of the system during changes in the environment, the optimization is included in the CANN-MPPT controller to fine tune the parameters of the network.

Woodpecker Mating Algorithm

Inspiration of WMA

The WMA is a nature-inspired metaheuristic optimization rule, which emulates the intelligent and drumming behaviour of woodpeckers. In the WMA rule, male woodpeckers drum to attract females, while the strength and fitness of a male woodpecker are reflected in the intensity and quality of the drumming sound. Whether a female woodpeckers responded and moved towards a sound depended on the quality of the sound produced, thereby forming a dynamic selection process. In WMA, any "population" with better "fitness" drew other population members toward itself search.

The WMA to optimally tune the parameters of a CANN-based MPPT controller flowchart illustrates in Fig. 7. WMA made modifications to the weights, connections and structure for the ANN that improve prediction accuracy and convergence speed, resulting in improved tracking of MPP under different irradiance and temperature.

Sound Intensity and Population Dynamics In WMA

Since sound intensity represents each male agent's fitness in WMA, greater intensity stands for better solution quality.

The female agents are drawn to males with an intense drumming sound, promoting the chance of selecting the best male agent.

By splitting the agents into two populations, male and female woodpeckers, and mimicking natural mating behavior to optimize solutions, explore a variety of ANN configurations, with the added benefit of tuning the network weights more effectively.

Numerical Implementation Of WMA

Step1: Initialization

WMA starts by initializing a population of candidate solutions (pairs of male and female woodpeckers), each representing sets of CANN-MPPT controller parameters (membership functions, learning rates, etc.). The candidates are uniformly and randomly distributed in the parameter space.

Step 2: Fitness Evaluation and movement

In each iteration, the population is ranked in order of fitness based on MPPT performance metrics, i.e., tracking efficiency, and every woodpecker (the solution) moves based on where the best male is using:

$$(W)^{m(x+1)} = W^{mx} + Rand * \Delta^t \qquad (21)$$

$$\Delta^t = \psi_{best} * \frac{(W_{xbest} - W_{it})}{2} + \Omega\eta^v \qquad (22)$$

Here, $(W)^{m(x+1)}$ denotes the location of the current woodpecker (i.e., test CANN parameter set) at iteration $x+1$, while W^{mx} is the location at iteration x. The term $Rand$ denotes random number in the range (0, 1), which creates some stochasticity in the update process to promote global search behavior. The term $\psi best$ is a learning coefficient appropriate to the best-performing CANN controller, like the most dominant male woodpecker. W_{xbest} stands location of best male woodpecker, while W_{it} stands current location of individual candidate at iteration ttt. The final term $\Omega\eta^v$, is a random coefficient vector.

Step 3: Influence of best solution on population

During the optimization process, the CANN controller, which is equivalent to the dominant male woodpeckers, produces the best control strategy and has an impact on the adjustment behaviour of the other candidate solutions (the female woodpeckers). Each CANN parameter vector updates its position in response to the best solution using the following expression:

$$W = Rand + Z \qquad (23)$$

Here, $Rand$ stands uniform random number in the interval (0,1) to add variability into the

update. The Z term is a dynamic parameter that changes throughout the iteration cycle; the use of Z is to constrain the variability between exploration and exploitation in the CANN parameter space.

Step 4: Convergence or diversification based on quality

If $W_i > 1$, female woodpeckers wander from the target woodpecker to search for further possible locations. Otherwise, they converge on the target woodpecker as follows:

$$\beta = \frac{1}{1+iten_n^m} \tag{24}$$

Here β represents behavioral influence of the male woodpecker (i.e., best CANN solution), and $iten_n^m$ is the sound intensity (i.e., the behavioral response function) associated with the target woodpeckers. To constrain this evolution over iterations of the algorithm, the parameter Z, which helps regulate exploration as well as convergence tendencies, expressed as:

$$Z = TSF + 1 - \left(\frac{iter}{iter_{max}}\right) \tag{25}$$

Where, TSF is a tangent sigmoid function to govern step behavior, $iter$ denotes present iteration number, and $iter_{max}$ denotes maximum number of iterations.

As the algorithm works through reduction in the number of active male candidates, which reduced adaptively for ending up with a more accurate solution, given as follows:

$$W_{male} = f\left(Cir\left(\frac{\pi}{2}\right)\cdot\left(\frac{iter}{iter_{max}}\right)\right) + 1 \tag{26}$$

Moreover, the current step size Δ^t for modifying the parameters while optimizing is determined as follows,

$$\Delta^t = \Psi_{best}\cdot\left(\frac{W_{xbest} - W_{it}}{2}\right) + \Omega\eta^v \tag{27}$$

Where, $\Psi best$ is the previous influence of the best CANN controller, W_{xbest} is the best CANN parameter vector up to that point, W_{it} is the current CANN candidate position, and $\Omega\eta^v$ stands random perturbation to create movement. Finally, there is an imposed threshold value that governs the movement dynamics on the sound intensity of the woodpeckers:

$$TH = \sum_{i=1}^{n-1}\left(\frac{W_{best}}{n-1}\right) \tag{28}$$

Where, TH indicates the average influence of the best solutions, which creates a random run-away movement to move away from local optima and is useful to promote convergence characteristics.

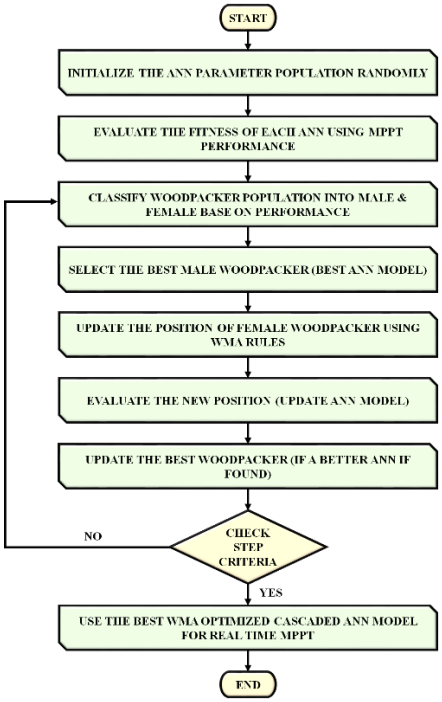

Fig.7. Flowchart of WMA-CANN-MPPT.

Step 5. Randon running away strategy

To avoid local optima during CANN parameter tuning, the Random Running Away (RRA) strategy updates the solution within defined bounds:

$$RRA = ib - (ib - ub)\cdot Rand \tag{29}$$

Where $ib\ and\ ub$ represents lower and upper boundaries of CANN parameters, and $Rand$ stands random number in (0,1). The Group Run Away (GRA) probability is calculated as:

$$GRA = \psi\cdot\left(\frac{iter}{iter_{max}}\right) \tag{30}$$

Where Ψ is a random coefficient, and r stands random value in (0,1). If GRA=1, this initiates a group-level escape and improve global search.

Step 6. Final position update and selection:

The new position of the female woodpecker (CANN candidate) determined by moving between its now current place and the new best performing solution:

$$W_{GRA} = W_{it} + GRA \cdot \left(\left\{ W_{best}^{t} - W_{j} \right\} \cdot Rand \right) \quad (31)$$

Where W_{it} the current position, W_{best}^{t} is the best CANN solution discovered, W_j is a randomly selected solution. If new position provided better MPPT performance, this replaces the previous position. After stopping condition (e.g. maximum iterations) has been achieved, the best solution becomes the optimal solution for the CANN controller. The CANN MPPT controller using WMA used to improve the tracking speed, accuracy under various dynamic situations and delivers a stable output DC power from PV system.

The regulated DC output power is stored in a DC-link capacitor and then efficiently changed into high-quality AC power with a 3φ VSI, which is discussed below.

D. Three Phase Inverter Connected To Grid Via Lc-Filter

The configuration of a 3φ VSI contains six switches $\left(S_1, S_2, S_3, \bar{S}_1, \bar{S}_2, \bar{S}_3\right)$ arranged to make three inverter branches as displays Fig. 8. Each inverter branch is a complementary switch pair $\left(S_1 \,\&\bar{S}_1\right), \left(S_2 \,\&\bar{S}_2\right), \left(S_3 \,\&\bar{S}_3\right)$, that creates a balanced 3 φ AC voltage from a DC input (V_{dc}). The inverter switches are switched via PWM techniques to control output voltage amplitude and frequency, and while PWM switching generates output at high frequency, it also produces voltage and current harmonics that affect overall power quality.

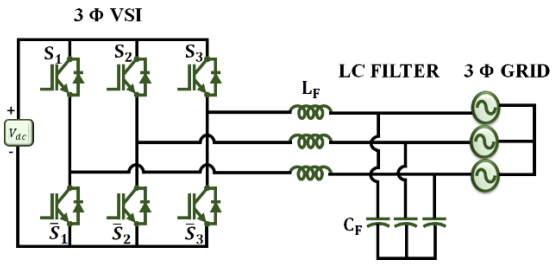

Fig. 8. 3 φ VSI connected to Grid via LC-filter.

As power quality hampered by the harmonic currents and voltages, it is convention to use an LC filter at the inverter output.

Fig. 9 shows PV system and converter's input stage, under constant conditions (case 1). PV panel remains a steady temperature of [ ] while the irradiance is set up at a constant condition of [ ] which ensure PV panel produced constant energy through the simulation run time. The input voltage to the step-up converter remained stable at [ ], while the input current steadily ramped up and finally stabilized around [ ].

The series inductors in the filter diminish the ripple current content by limiting the high-frequency energy in the output current, while the parallel capacitor delivers a low-impedance path to ground for high-frequency voltage harmonic components. Therefore, the LC filter action results in a smooth, sinusoidal output current deliver to the grid. The inverter output voltages are filtered with the LC network to suppress harmonics and exchange clean sinusoidal waveforms with the grid by regulating active and reactive power and maintaining power quality.

IV. RESULT AND DISCUSSIONS

In this section, a X^2W step-up converter with a WMA-CANN MPPT controller developed and simulated in MATLAB for a PV-based grid system. The simulation done to observe the performance of converter and controller. The specification of PV system and proposed converter are detailed in Table 1.

Table 1

Parameter Specifications

Parameters	Specifications
PV system	
Open Circuit Voltage	37.25*V*
Short Circuit Voltage	8.95*V*
Series Connected PV cell	3
Parallel Connected PV cell	13
Maximum Power Voltage	29.95*V*
Rated Power	10*kW*
X^2W Step-Up converter	
Switching Frequency	10*KHz*
L_a, L_p, L_s	4.7 *mH*
L_k, L_m	45*mH*
C_a, C_b	22μF
C_0	2200μF

Case 1: Constant Condition

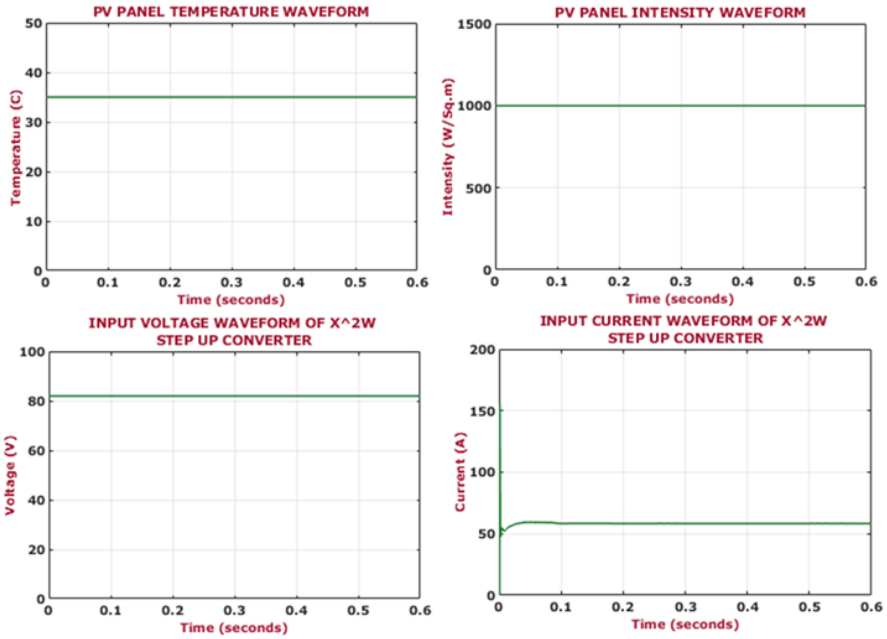

Fig.9. Characteristics waveforms of PV panel under case 1.

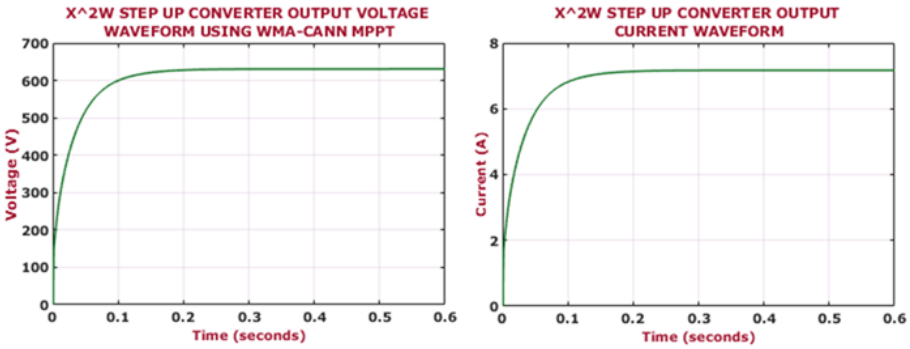

Fig.10. Converter output waveforms under case 1.

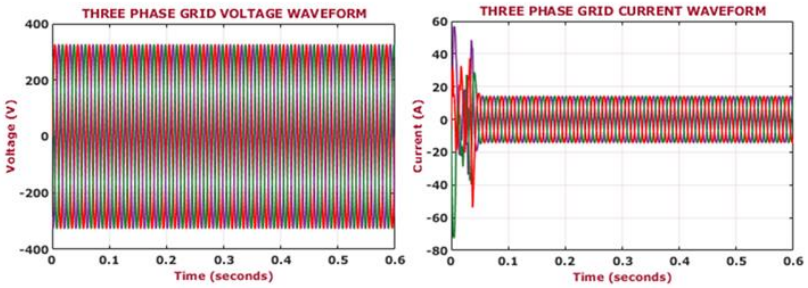

Fig.11. Three phase grid waveforms under case 1.

Fig. 10 displays output response of WMA-optimized CANN MPPT controlled X^2W step-up converter under case 1. The output voltage rapidly rises to settle at $690V$, demonstrating effective voltage boosting. The converter's output current recorded rises and then remains virtually steady at

close to $8A$, demonstrating the effectiveness of the optimized controller that operates to maintain maximum power extraction from the PV source in unchanging ambient conditions.

Fig. 11 displays 3 φ current and voltage waveforms at the grid side under case 1. The voltage waveform maintains a symmetric sinusoidal pattern around $\pm 300V$ across all phases. From there, the current waveform undergoes an initial transient effect before sharply stabilizing to symmetrical waveforms with peak values of around $\pm 20A$, demonstrates strong synchronization with the grid and smooth power transfer.

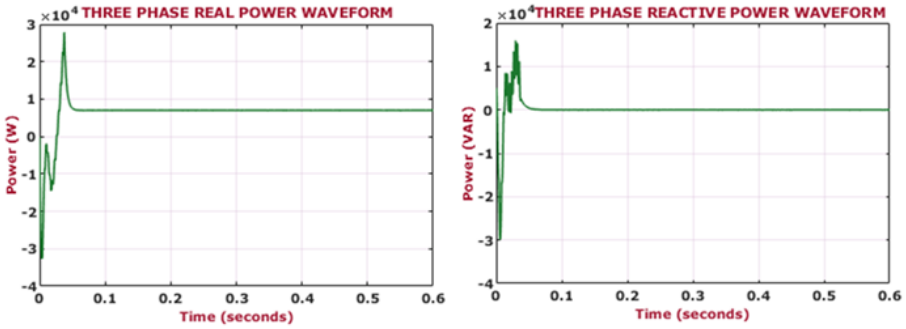

Fig.12. Real and Reactive waveforms under case 1.

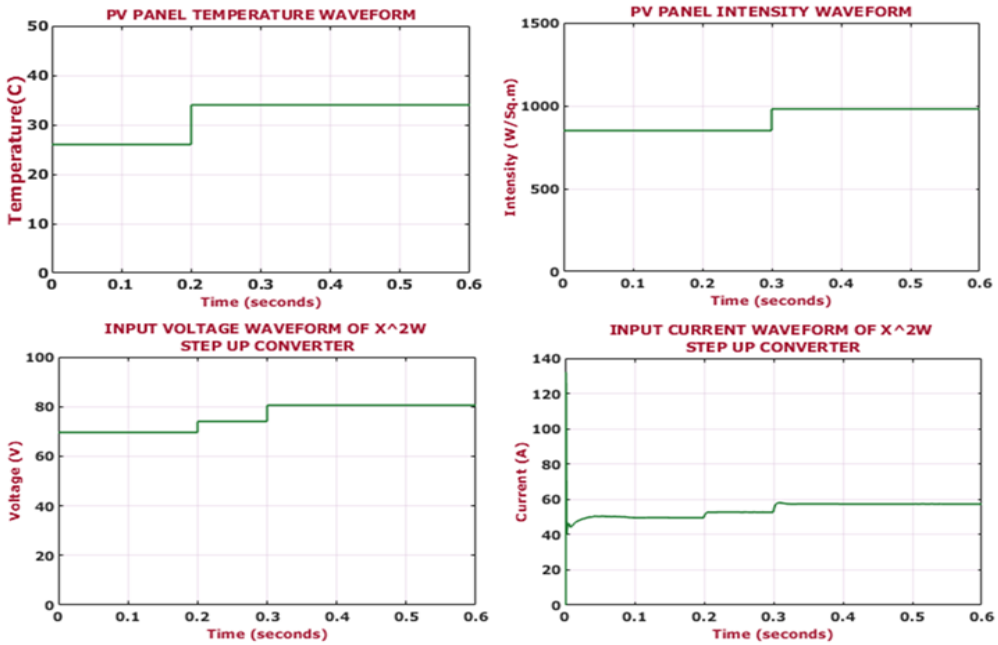

Fig.13. Characteristics waveforms of PV panel under case 2.

Fig. 12 shows the 3 φ power characteristics under constant operating conditions (case 1). The real power waveform has a short-term transient initially and subsequently continues a stable waveform indicating the accurate and stable real power delivered into the grid. The reactive power waveform exhibits initial transient behaviour, but quickly stabilizes to a level close to reference. This response indicates that the system maintains transient reactive power exchange to a minimum and operate efficiently, which contributes to enhanced grid stability and system operation.

Case 2. Varying Condition

Fig. 13 shows the effects of changing ambient conditions on the PV panel and the converter input side under case 2. The PV panel is located at a temperature of $25°C$ and an irradiance of $850W/m^2$. After 0.2 s and 0.3 s both temperature and irradiance increase; thus, the temperature rises to $35°C$ and the irradiance rises to $1000W/m^2$. The converter input voltage rises from $70V$ *to* $90V$ and the input current increases from $50A$ *to* $65A$. As these results illustrate, the system react to changing external conditions

quickly and return to a relatively stable input within reasonable timeframes, while still receiving maximum energy from the PV source.

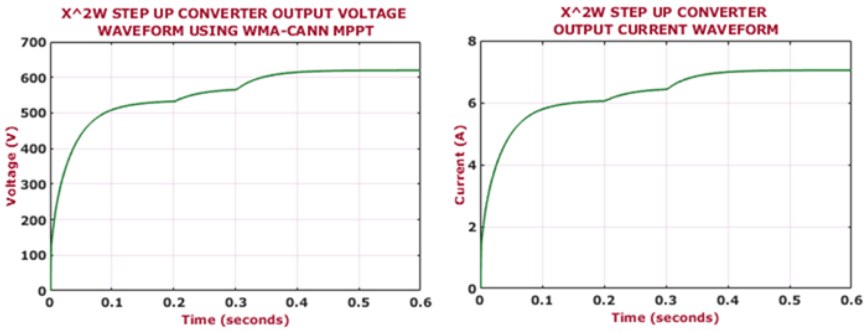

Fig.14. Converter output waveforms under case 2.

Fig. 14 shows output characteristics from the X^2W step-up converter under changing condition (case 2) used with the WMA-CANN MPPT strategy. As temperature and irradiance steadily increases, the converter output voltage had increased from $550V$ to about $690V$, where the transition followed a stable path after 0.25 s. The *Case 3. Load Changes* output current increased from $6A to 8A$, is generally following the same transition as the input condition. The results indicate an effective tracking response of the optimized controller, therefore supporting the converter dynamically adjusting maximized output to the grid in the changing input weather.

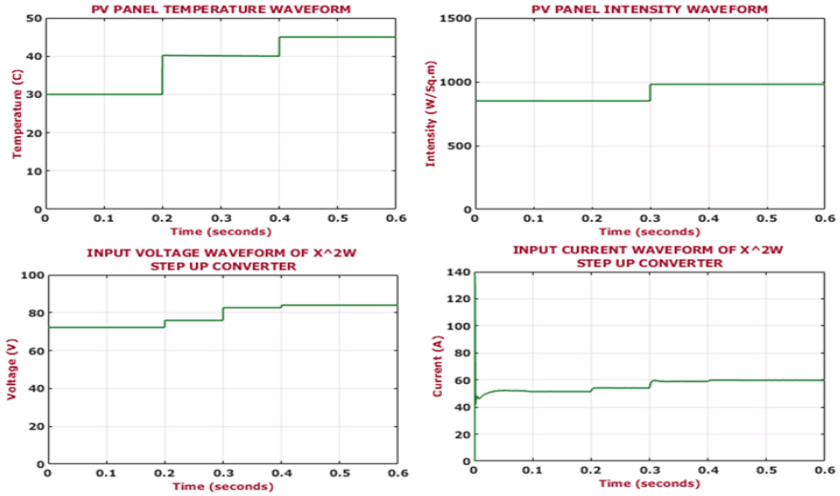

Fig.15. Characteristics waveforms of PV panel under case 3.

Fig. 15 represents performance of PV panel and step-up converter input parameters during case 3 dynamic load conditions. The PV panel temperature, which stepped from $30°C to 40°C$ at 0.3 s, and then to $45°C$ at 0.4 s. This series of changes to PV temperature reflects the accumulative effects of the increasing ambient thermal conditions. The profile of solar irradiance stepped at 0.3 s from $850W/m^2 to 1000W/m^2$ to simulate the increased availability of sunlight. As a result of the environmental and load changes, the input voltage and input current waveforms of the X^2W step-up converter both increased; the input voltage increased from $70V to 90V$, and input current increased from approximately $45A to 55A$.

These variations indicate the operational commitment of the system's adaptive power tracking capabilities when environmental and load changes are present.

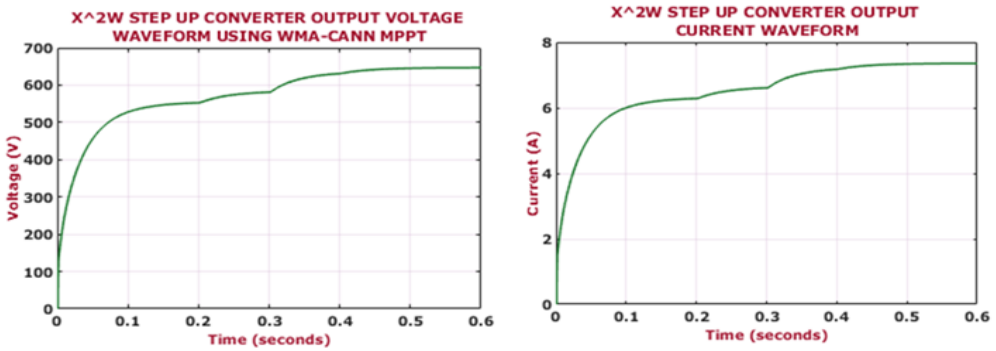

Fig.16. Converter output waveforms under case 3.

Fig. 16 illustrates the output characteristics of the X^2W step-up converter, controlled via the WMA-CANN MPPT control technique, under the load variation condition. The load voltage, stabilizes from $100V\,to\,690V$ in less than 0.1s, and then gradually smooths as irradiance and temperature dynamically change. The load current ramps steadily to $8A$, demonstrating a noticeable step in behaviour through the input variation.

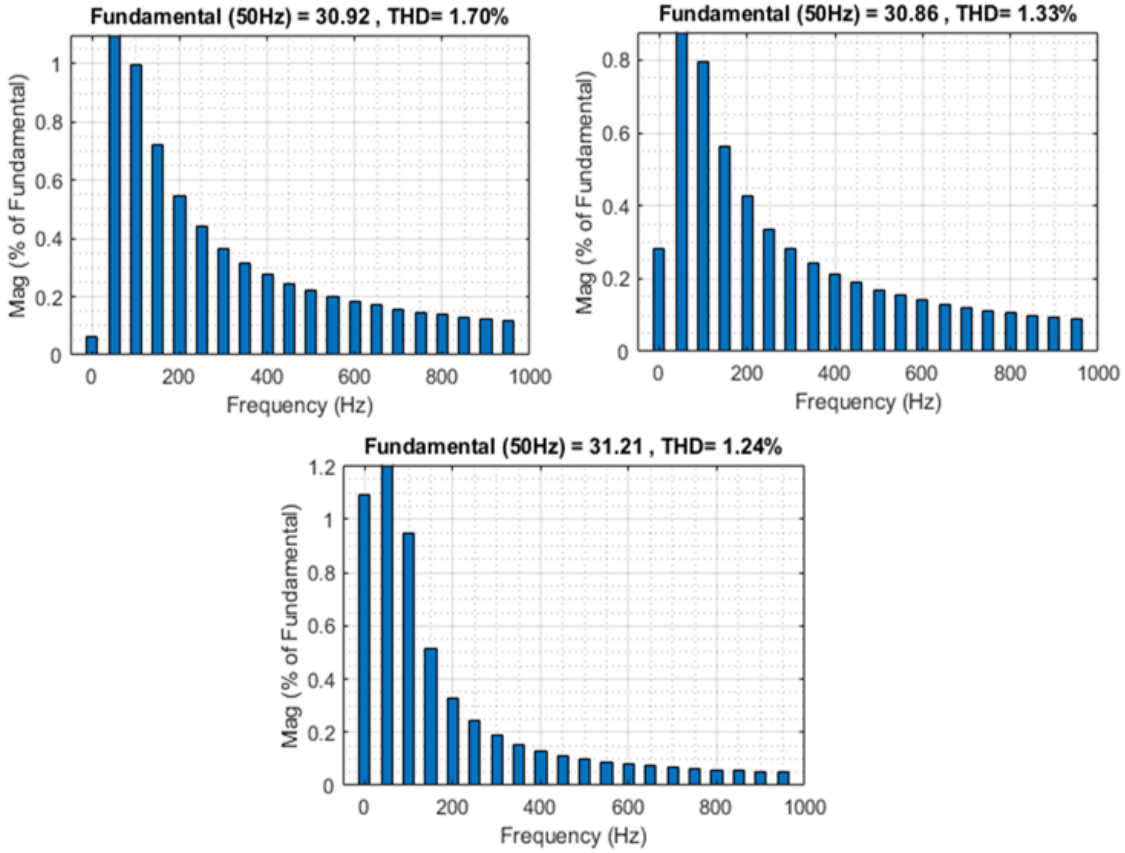

Fig.17. 3 φ THD waveforms.

Fig. 17 represents the hormonic spectra of B, R, and Y phase waveforms, showing the basic frequencies at $50Hz$ with corresponding THD values of 1.70%, 1.33%, and 1.24%. The Y phase exhibits a lowest distortion, which suggest better hormonic suppression and waveform quality across the 3 φ system.

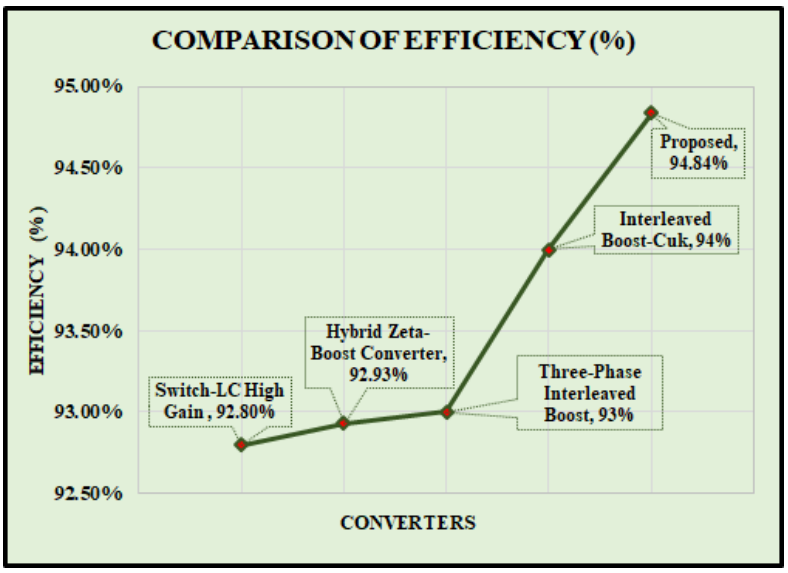

Fig.18. Comparison of Converter Efficiency.

Fig. 18 illustrates efficiency of various converters: Switch LC based High Gain (SLCHG) converter reaches 92.80% [20], Hybrid Zeta Boost (HZB) converter reaches 92.93% [21], Three-phase Interleaved Boost converter reaches 93% [10], Interleaved Boost-Cuk (IBC) converter reaches 94% [22], and the proposed converter reaches a maximum of 94.84% efficiency. The proposed design has a greater efficiency able to convert a larger amount of input power into usable output power without losses, showing efficient energy allocation, and a reduction in long-term utility costs.

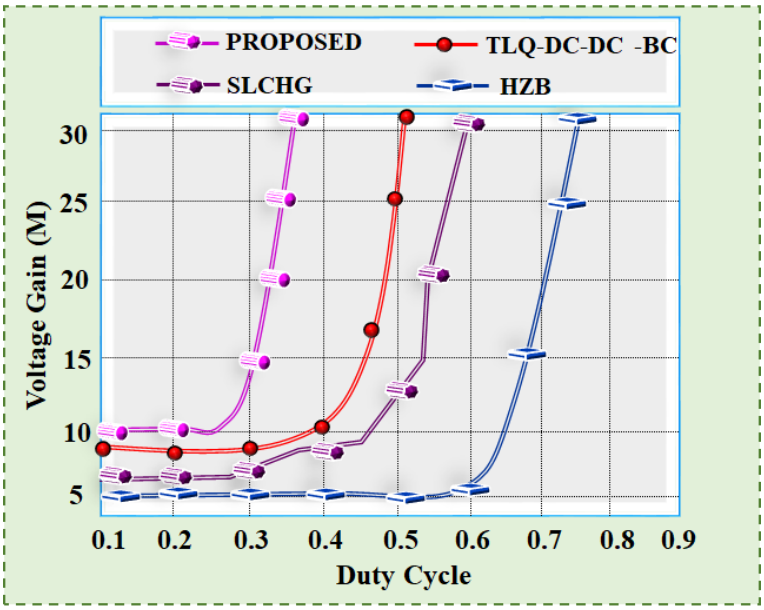

Fig.19. Comparison of Converter Voltage Gain.

Fig. 19 shows voltage gain versus duty cycle for TLQ-DC-DC-BC [12], SLCHG [20], HZB [21] and proposed converter. The proposed converter offers much greater voltage gain as duty cycle is increased compared to the other converters. The result shows the proposed converter produce greater output voltage even at low duty cycles making it the better choice for efficiency overall.

Table 2

Comparison of Converter Components

Converter	Switches	Diode	Inductor	Capacitor	Total Component
SLCHG [20]	2	6	2	4	14
TLQ-DC-DC-BC [12]	1	7	2	6	16
HZB [21]	2	8	5	3	18
PROPOSED	1	3	5	3	12

In Table 2, the number of components utilized in various converter topologies is shown. The proposed converter uses only 12 components, which is less than SLCHG [18], TLQ-DC-DC-BC [12] and HZB [21]. Fewer components result in lower cost, less circuit complexity, and improved reliability. As a result, the proposed design is more effective and practical for implementation.

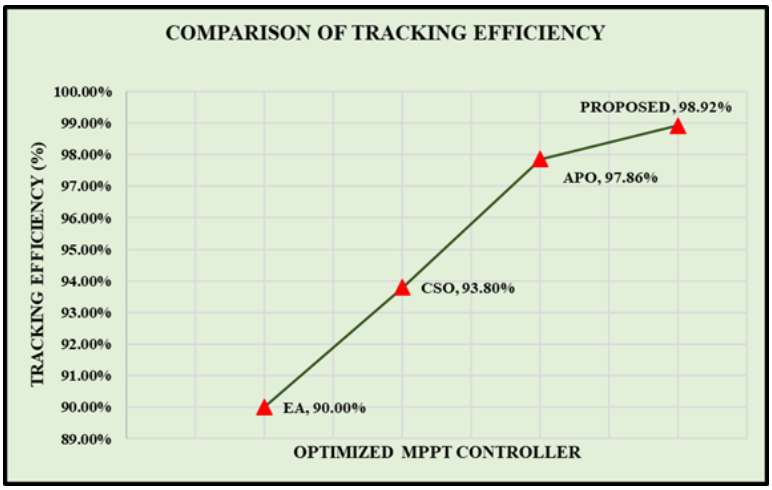

Fig.20. Comparison of Optimized MPPT Controller Tracking Efficiency.

Fig. 20 compares tracking efficiency of different optimized MPPT controllers. EA-optimized [17] controller achieved 90%, Cuckoo Search-Optimized (CSO) [23] controller achieved 93.8% and Advanced Perturb & Observation (APO) [24] algorithm-based controller achieved 97.86%. The proposed controller achieved the highest tracking efficiency at 98.92%. This efficiency distinguishes the proposed controller due to its capability to track MPP more swiftly and accurately compared than other controllers in the presence of dynamic ecological circumstances.

V. CONCLUSION

This work develops a highly efficient PV energy conversion system including a X^2W step-up converter and WMA optimized CANN-MPPT controller for dynamic grid connected applications.

The step-up converter highly achieved better voltage gain with fewer components and better affordability.

Using a WMA based CANN MPPT controller, the MPPT performance significantly improved to an overall tracking efficiency of 98.92%, while also achieving fast convergence and tracking performance under different irradiance and loads. The MATLAB simulation outcomes demonstrated the capability of system to achieve stable output power and reduced harmonic distortions, with a THD of only 1.24%, as well as achieving a peak efficiency of 94.84% for the converter. The proposed system is highly illustrative of a real-time fully integrated MPPT solar PV energy conversion system, which proves to be a feasible and contemporary solution for smart and sustainable PV-grid integration.

REFERENCES

[1] Tawfiq A.A.E., El-Raouf M.O.A., Mosaad M.I., Gawad A.F.A., Farahat M.A.E. Optimal reliability study of grid-connected PV systems using evolutionary computing techniques. *IEEE Access*, 2021, vol. 9, pp. 42125-42139.

[2] Kiran S.R., Basha C.H., Singh V.P., Dhanamjayulu C., Prusty B.R., Khan B. Reduced simulative performance analysis of variable step size ANN based MPPT techniques for partially shaded solar PV systems. *IEEE access*, 2022, vol. 10, pp. 48875-48889.

[3] Bhukya L., Kedika N.R., Salkuti S.R. Enhanced maximum power point techniques for solar photovoltaic system under uniform insolation and partial shading conditions: a review. *Algorithms*, 2022, vol. 15, no. 10, pp. 365.

[4] Gunapriya B., Abinaya I., Karthik M., Vidhya H. Anti-windup PI controller with tracking for motor drive system: Modelling, simulation and implementation in lab view based FPGA, *International Journal of Recent technology and Engineering*. vol. 8, no. 5.

[5] Abinaya, I., Gowsika M., Jothika, S. P., Dharini K., Vidhya H. Smart Monitoring of Carbon Monoxide using Internet of Things International Journal of Innovative Technology and Exploring Engineering (IJITEE), 2020, vol. 9, no. 3.

[6] Uthirasamy R., Chinnaiyan V.K., Vishnukumar S., Karthick A., Mohanavel V., Subramaniam U., Muhibbullah M. Design of Boosted Multilevel DC-DC Converter for Solar Photovoltaic System. *International Journal of Photoenergy*, 2022, no. 1, pp. 1648474.

[7] Kavin K.S., Subha Karuvelam P., Devesh Raj M., Sivasubramanian M. A novel KSK converter with machine learning MPPT for PV applications. *Electric power components and systems*, 2024, pp. 1-19.

[8] Kavin K.S., Karuvelam P.S. Matcha M., Vendoti S. Improved BRBFNN-based MPPT algorithm for coupled inductor KSK converter for sustainable PV system applications. *Electrical Engineering*, 2025, pp. 1-23.

[9] Ertekin D. A high gain switched-inductor-capacitor DC-DC boost converter for photovoltaic-based micro-grid applications. *CSEE Journal of Power and Energy Systems*, 2023.

[10] Pirashanthiyah L., Edirisinghe H.N., De Silva W.M.P., Bolonne S.R.A., Logeeshan V., Wanigasekara C. Design and analysis of a three-phase interleaved DC-DC boost converter with an energy storage system for a PV system. *Energies*, 2024, vol. 17, no. 1, pp. 250.

[11] Hayat A., Sibtain D., Murtaza A.F., Shahzad S., Jajja M.S., Kilic H., Design and analysis of input capacitor in DC–DC boost converter for photovoltaic-based systems. *Sustainability*, 2023, vol. 15, no. 7, pp. 6321.

[12] Belhadj S.M., Meliani B., Benbouhenni H., Zaidi S., Elbarbary Z.M.S., Alammar M.M. Control of multi-level quadratic DC-DC boost converter for photovoltaic systems using type-2 fuzzy logic technique-based MPPT approaches. *Heliyon*, 2025, vol. 11, no. 3.

[13] Ibrahim M.H., Ang S.P., Dani M.N., Rahman M.I., Petra R., Sulthan S.M. Optimizing step-size of perturb & observe and incremental conductance MPPT techniques using PSO for grid-tied PV system. *IEEE access*, 2023, vol. 11, pp. 13079-13090.

[14] Dehghani M., Taghipour M., Gharehpetian G.B., Abedi M. Optimized fuzzy controller for MPPT of grid-connected PV systems in rapidly changing atmospheric conditions. *Journal of Modern Power Systems and Clean Energy*, 2020, vol. 9, no. 2, pp. 376-383.

[15] Almutairi A., Abo-Khalil A.G., Sayed K., Albagami N. MPPT for a PV grid-connected system to improve efficiency under partial shading conditions. *Sustainability*, 2020, vol. 12, no. 24, pp. 10310.

[16] EL-Banna M.H., Hammad M.R., Megahed A.I., Aboras K.M., Alkuhayli A., Gowtham N. On-grid optimal MPPT for fine-tuned inverter based PV system using golf optimizer considering partial shading effect. *Alexandria Engineering Journal*, 2024, vol. 103, pp. 180-196.

[17] Mendez-Flores E., Ortiz A., Macias I., Molina A. Experimental validation of an enhanced MPPT algorithm and an optimal DC–DC converter design powered by metaheuristic optimization for PV systems. *Energies*, 2022, vol. 15, no. 21, pp. 8043.

[18] Esmaeili, Soroush, Sara Hasanpour, and Hossein Hafezi. "New high step-up coupled dual winding quadratic enhanced SEPIC DC-DC converter." In 2021 International Conference on Smart Energy Systems and Technologies (SEST), pp. 1-6. IEEE, 2021.

[19] Danyali, Saeed, Rahmat Aazami, Amin Moradkhani, and Mostafa Haghi. "A new dual-input three-winding coupled-inductor based DC-DC boost converter for renewable energy applications." International Transactions on Electrical Energy Systems 31, no. 1 (2021): e12686.

[20] Kumar A., Wang Y., Pan X., Raghuram M., Singh S.K., Xiong X., Tripathi A.K. Switched-LC based high gain converter with lower component count. *IEEE transactions on industry applications*, 2020, vol. 56, no. 3, pp. 2816-2827.

[21] Bhaskar M.S., Gupta N., Selvam S., Almakhles D.J., Sanjeevikumar P., Ali J.S.M., Umashankar S. A new hybrid zeta-boost converter with active quad switched inductor for high voltage gain. *IEEE Access*, 2021, vol. 9, pp. 20022-20034.

[22] Preethiraj P.M. Maximum power point tracking in fuel cells an AI controller based on metaheuristic optimisation. *Scientific Reports*, 2024, vol. 14, no. 1, pp. 31955.

[23] Mariprasath T., Basha C.H., Khan B., Ali A. A novel on high voltage gain boost converter with cuckoo search optimization based MPPTController for solar PV system. *Scientific reports*, 2024, vol. 14, no. 1, pp. 8545.

[24] Raj A., Praveen R.P. Highly efficient DC-DC boost converter implemented with improved MPPT algorithm for utility level photovoltaic applications. *Ain Shams Engineering Journal*, 2022, vol. 13, no. 3, pp. 101617.

Information about authors.

Mr. T. Amar Kiran, MD His main area of interest includes Power Quality and Micro grid.
Email: amarkiran@giet.ac.in
https://orcid.org/0000-0002-3021-1453

Madireddy Sridhar studying in department of Electrical and Electronics Engineering in Godavari Institute of Engineering and Technology from Jawaharlal Nehru Technological University, Kakinada. His main area of interest includes Power Quality and Power Electronics.
Email: sridharmadhireddy750@gmail.com
https://orcid.org/0009-0008-1286-7011

Lakkoju Manikanth studying in department of Electrical and Electronics Engineering in Godavari Institute of Engineering and Technology from Jawaharlal Nehru Technological University, Kakinada. His main area of interest includes Power Quality and Power Electronics.
Email: kanthmanikanth5@gmail.com
https://orcid.org/0009-0006-6740-6621

Mrs. **K. Gowtami, MD.**
Her main area of interest includes Power Electronics and Electrical Machines.
Email: gowthami75.k@gmail.com
https://orcid.org/0000-0002-1166-5687

Madduri Mohan Sai Durga Ramesh studying in the Department of Electrical and Electronics Engineering in Godavari Institute of Engineering and Technology from Jawaharlal Nehru Technological University, Kakinada. His main area of interest includes Power Quality and Power Electronics.
Email: rameshmadduri322@gmail.com
https://orcid.org/0009-0001-8479-5781